

Thermal Properties of Mixed Alkali Bis(trifluoromethylsulfonyl)amides

Rika Hagiwara,* Kenichiro Tamaki, Keigo Kubota, Takuya Goto, and Toshiyuki Nohira

Graduate School of Energy Science, Kyoto University, Sakyo-ku, Kyoto 606-8501, Japan

Phase diagrams of binary mixtures of alkali bis(trifluoromethylsulfonyl)amides have been constructed, and their eutectic compositions and temperatures have been determined. It has been revealed that the molten salt electrolytes having the melting points in the intermediate temperature range (373 to 473) K are easily formed by simple mixing of two kinds of single alkali bis(trifluoromethylsulfonyl)amide salts. The 1:1 or 3:1 double salt is occasionally formed for some binary systems.

Introduction

Molten salts have excellent characteristics as electrolytes such as negligibly small volatility, nonflammability, high electrochemical stability, and high ionic conductivity.^{1,2} Molten salts are roughly classified into two groups: high-temperature molten salts ($T > 673$ K) and room (or ambient) temperature molten salts ($T < 373$ K). There is a tradeoff between the features as electrolytes for high-temperature and room-temperature molten salts. High-temperature molten salts are generally superior in physicochemical properties such as high conductivities, wide electrochemical windows, and wide liquid temperature range. On the other hand, room-temperature molten salts, also called ionic liquids, have the advantages of an easy handling and wide range of application field.^{3–6} Salts consisting of alkali metal cations and the bis(trifluoromethylsulfonyl)amide (Tf_2N) anion, MTf_2N ($M = \text{Li, Na, K, Rb, Cs}$), are solids at room temperature but have, or are expected to have, melting points at relatively low temperatures.^{7,8} The Tf_2N anion is well-known as one of the major anions constituting room-temperature molten salts because of its high chemical and electrochemical stability.⁹

It would be possible to obtain molten salts having melting points of lower than those of the single MTf_2N salts from their mixture. These molten salt mixtures are expected to have melting points from (373 to 473) K and be used at intermediate temperatures (373 to 673) K, giving averaged characteristics of high-temperature and room-temperature molten salts. It is also expected that the alkali metal Tf_2N salts are promising as intermediate temperature molten salt electrolytes for electrochemical systems including a process of alkali metal depositions owing to the high electrochemical stability of the Tf_2N anion. For example, lithium metal is expected to deposit at the cathode limit of mixed MTf_2N molten salts containing LiTf_2N , and these molten salts are able to be used as electrolytes for lithium ion batteries operating at intermediate temperatures.

Many researchers have reported organic electrolytes for lithium ion batteries in which LiTf_2N is dissolved as supporting electrolytes;^{10–12} however, the properties reported for MTf_2N salts themselves are limited except for some crystal structures.¹³ No reports are available on the physicochemical properties of the molten MTf_2N salts and their mixtures.

In this study, the thermal properties of the mixtures of the two MTf_2N single salts ($M = \text{Li, Na, K, Rb, Cs}$) were

Table 1. Melting Temperature, T , and Decomposition Temperatures, T_d , of MTf_2N Single Salts

	LiTf_2N	NaTf_2N	KTf_2N	RbTf_2N	CsTf_2N
T/K (this study)	506	530	472	450	395
T/K (previous study)	507 ⁷	—	478 ⁷	—	388 ⁸
T_d/K	657	714	733	740	745

systematically investigated to construct phase diagrams and determine the composition giving the melting points in the intermediate temperature range.

Experimental Section

Bis(trifluoromethylsulfonyl)imide, HTf_2N (Morita Chemical Industries, purity > 99 %), Na_2CO_3 (Wako Pure Chemical Industries, purity > 99.5 %), K_2CO_3 (Wako Pure Chemical Industries, purity 99.9 %), Rb_2CO_3 (Wako Pure Chemical Industries, purity 99.9 %), and Cs_2CO_3 (Aldrich, purity 99.9 %) were used for the syntheses of MTf_2N salts. LiTf_2N (Morita Chemical Industries, purity > 99.0 %) was used as received. Melting points and thermal decomposition temperatures of single MTf_2N salts were measured by means of differential scanning calorimetry (DSC) and thermogravimetry (TG), respectively. Temperature was increased with a scan rate of $10 \text{ K} \cdot \text{min}^{-1}$. The phase diagrams of the binary MTf_2N salt mixtures were constructed by plotting the temperatures of endothermic peaks found on the DSC curves obtained in the heating process against the compositions of the salts. The transition temperatures were determined in a heating process to avoid uncertainty by supercooling. The liquidus and solidus curves were drawn by eye through experimental plots. The measurement was performed for every five mole percent of the entire composition range. Aluminum pans were used for the sample holders. Prior to the measurements, the sample was melted at 573 K to prepare homogeneous samples. The measurement was started after cooling the pretreated samples to room temperature. In this study, the accuracy of melting points is ± 5 K.

Results and Discussion

Melting and Thermal Decomposition Temperatures of Single MTf_2N Salts. The melting and thermal decomposition temperatures of MTf_2N single salts in this study are summarized in Table 1. Figure 1 shows the plots of the melting points of the single salts against the reciprocal radii of the cations. Coordination numbers of the cations (LiTf_2N , 6; NaTf_2N , 6;

* Corresponding author. E-mail: hagiwara@energy.kyoto-u.ac.jp.

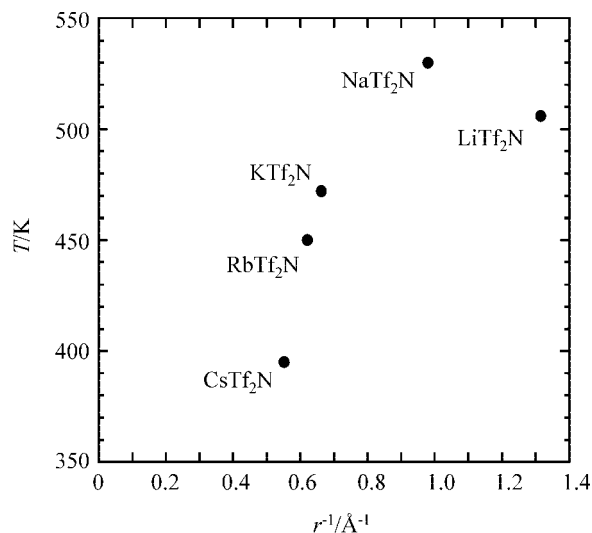


Figure 1. Plots of the melting temperature, T , against the reciprocal radius of the cations of the salts, r .

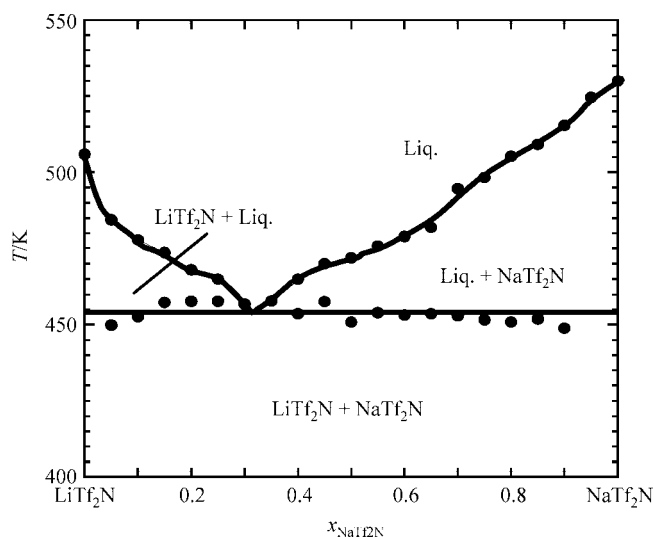


Figure 2. Phase diagram of $\text{LiTf}_2\text{N} + \text{NaTf}_2\text{N}$.

KTf_2N , 8; RbTf_2N , 8; CsTf_2N , 10) from the previous study on the crystal structure of the MTf_2N salts¹³ are used to estimate the Shannon's ionic radii of the cations. The melting point of the salt containing a smaller cation is generally higher, but it is found from the figure that the melting point of LiTf_2N does not follow the trend, irregularly lower than that of NaTf_2N . This would be caused by the difference of the lattice energies of the salts with different structures containing a large organic anion in which the electrostatic interactions are more complicated than that in simple inorganic salts. The single MTf_2N salts are thermally stable to 700 K except for LiTf_2N , which has a decomposition temperature of 657 K. Thermal stability becomes higher with the increase of the size of the cation.

Phase Diagrams of the Binary MTf_2N Salt Mixtures. Figure 2 shows a phase diagram of the $\text{LiTf}_2\text{N} + \text{NaTf}_2\text{N}$ binary system that exhibits a simple binary eutectic system. Figure 3 shows a phase diagram of the $\text{NaTf}_2\text{N} + \text{RbTf}_2\text{N}$ binary system. The phase diagram is also a simple eutectic type. No binary compounds and structural phase transitions are observed. These two systems are a simple eutectic type in the binary MTf_2N systems examined here.

Figure 4 shows a phase diagram of $\text{KTf}_2\text{N} + \text{CsTf}_2\text{N}$. There are two endothermic peaks on the DSC curves at different

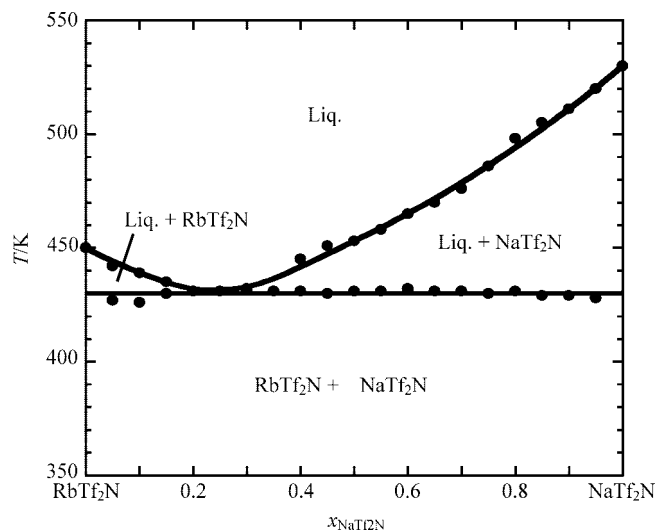


Figure 3. Phase diagram of $\text{NaTf}_2\text{N} + \text{RbTf}_2\text{N}$.

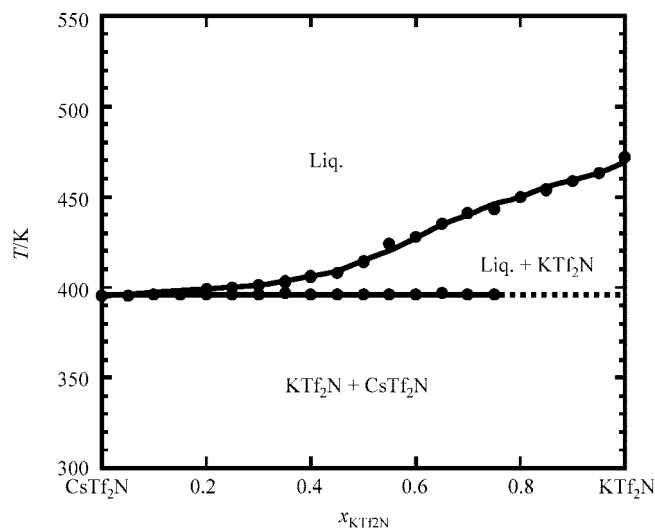
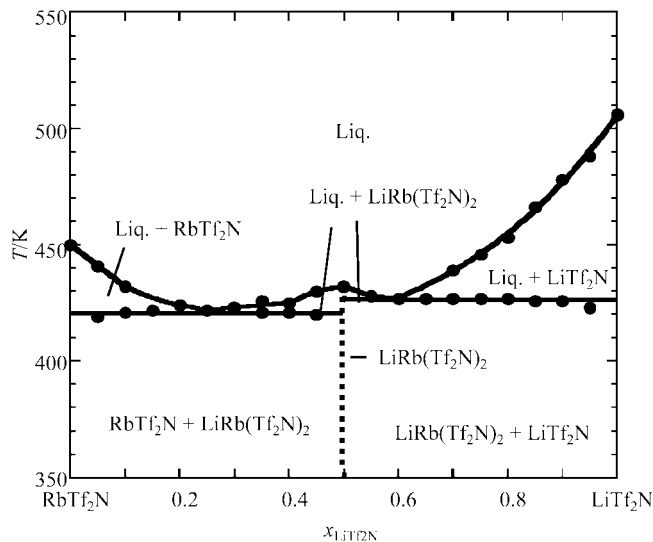
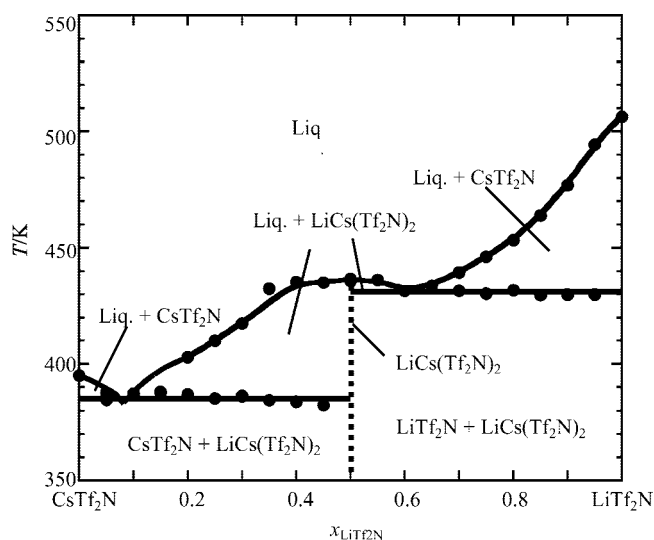
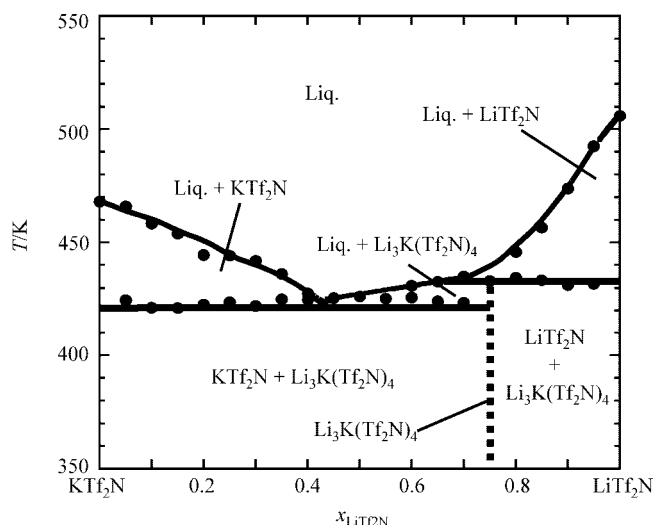


Figure 4. Phase diagram of $\text{KTf}_2\text{N} + \text{CsTf}_2\text{N}$.

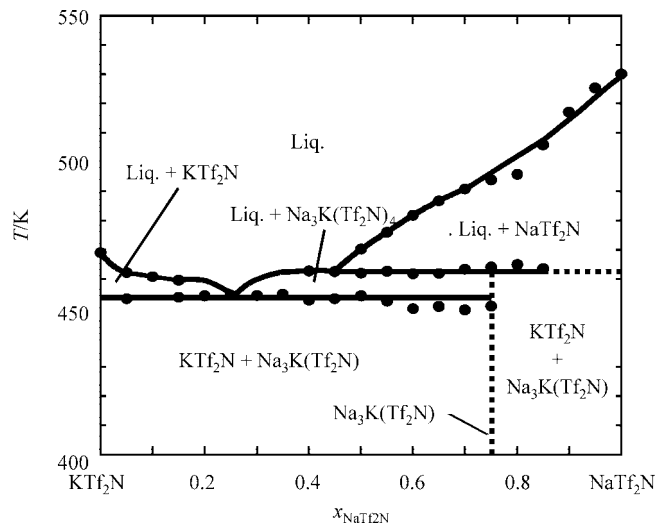
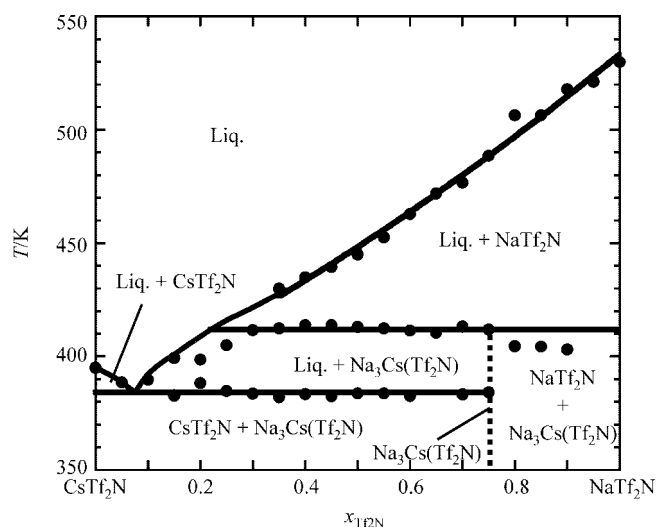
temperatures at $x_{\text{KTf}_2\text{N}} \geq 0.25$. Although only one peak is observed at $x_{\text{KTf}_2\text{N}} \leq 0.20$, the system is considered to be a eutectic type. It is considered that the eutectic composition is very close to the CsTf_2N side and that the eutectic temperature is almost equal to the melting point of neat CsTf_2N .

Figure 5 illustrates a phase diagram of the $\text{LiTf}_2\text{N} + \text{RbTf}_2\text{N}$ system. The endothermic peak found at the lowest temperature, 421 K, shifts by 5 K to a higher temperature, 426 K, at $x_{\text{LiTf}_2\text{N}} > 0.50$. At this composition, only one endothermic peak is observed at 432 K. This suggests the existence of a double salt, $\text{LiRb}(\text{Tf}_2\text{N})_2$. As a result, this binary system has two eutectic points. A similar phase diagram is found for the $\text{LiTf}_2\text{N} + \text{CsTf}_2\text{N}$ binary system as shown in Figure 6. The endothermic peak at 385 K appears only at the compositions where the molar ratios of LiTf_2N are 0.05 to 0.50, and this peak disappears for the higher LiTf_2N compositions. This suggests the existence of a double salt, $\text{LiCs}(\text{Tf}_2\text{N})_2$. As a result, this binary system has two eutectic points in common with $\text{LiTf}_2\text{N} + \text{RbTf}_2\text{N}$. Formation of 1:1 double salts is suggested for these two systems.

A phase diagram of the $\text{LiTf}_2\text{N} + \text{KTf}_2\text{N}$ binary system is shown in Figure 7. Two endothermic peaks are observed when the molar ratio of LiTf_2N exceeds 0.75. These observations suggest the existence of the 3:1 double salt, $\text{Li}_3\text{K}(\text{Tf}_2\text{N})_4$. A

Figure 5. Phase diagram of $\text{LiTf}_2\text{N} + \text{RbTf}_2\text{N}$.Figure 6. Phase diagram of $\text{LiTf}_2\text{N} + \text{CsTf}_2\text{N}$.Figure 7. Phase diagram of $\text{LiTf}_2\text{N} + \text{KTf}_2\text{N}$.

peritectic point should exist at $x_{\text{LiTf}_2\text{N}} \approx 0.7$ with the temperature of 435 K. The eutectic point is found at $x_{\text{LiTf}_2\text{N}} = 0.43$ with the temperature of 423 K. A similar phase diagram is obtained for the $\text{NaTf}_2\text{N} + \text{KTf}_2\text{N}$ binary system and shown in Figure 8.

Figure 8. Phase diagram of $\text{NaTf}_2\text{N} + \text{KTf}_2\text{N}$.Figure 9. Phase diagram of $\text{NaTf}_2\text{N} + \text{CsTf}_2\text{N}$.Table 2. Eutectic Compositions, x_{eu} , and Temperatures, T_{eu} , of the Binary MTf_2N Salt Mixtures

system	x_{eu}	T_{eu}/K
$\text{LiTf}_2\text{N} + \text{NaTf}_2\text{N}$	$x_{\text{LiTf}_2\text{N}} = 0.67$	453
$\text{LiTf}_2\text{N} + \text{KTf}_2\text{N}$	$x_{\text{LiTf}_2\text{N}} = 0.43$	423
$\text{KTf}_2\text{N} + \text{CsTf}_2\text{N}$	—	395
$\text{LiTf}_2\text{N} + \text{RbTf}_2\text{N}$	$x_{\text{LiTf}_2\text{N}} = 0.25$	421
	$= 0.60$	426
$\text{LiTf}_2\text{N} + \text{CsTf}_2\text{N}$	$x_{\text{LiTf}_2\text{N}} = 0.07$	385
	$= 0.60$	432
$\text{NaTf}_2\text{N} + \text{KTf}_2\text{N}$	$x_{\text{NaTf}_2\text{N}} = 0.25$	456
$\text{NaTf}_2\text{N} + \text{RbTf}_2\text{N}$	$x_{\text{NaTf}_2\text{N}} = 0.25$	431
$\text{NaTf}_2\text{N} + \text{CsTf}_2\text{N}$	$x_{\text{NaTf}_2\text{N}} = 0.07$	383

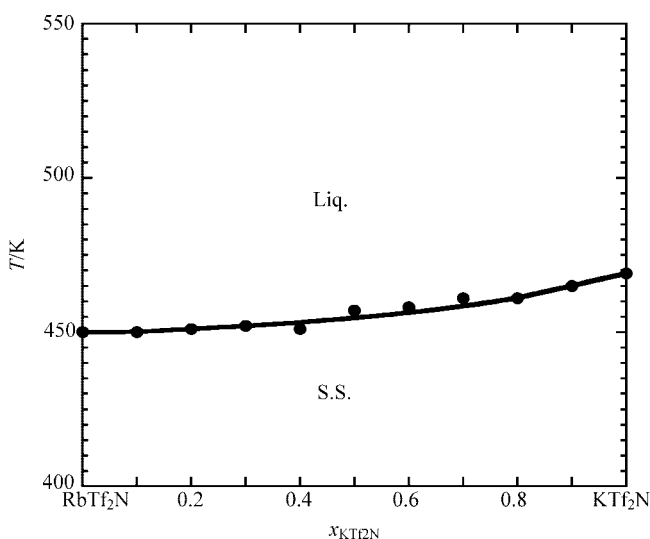
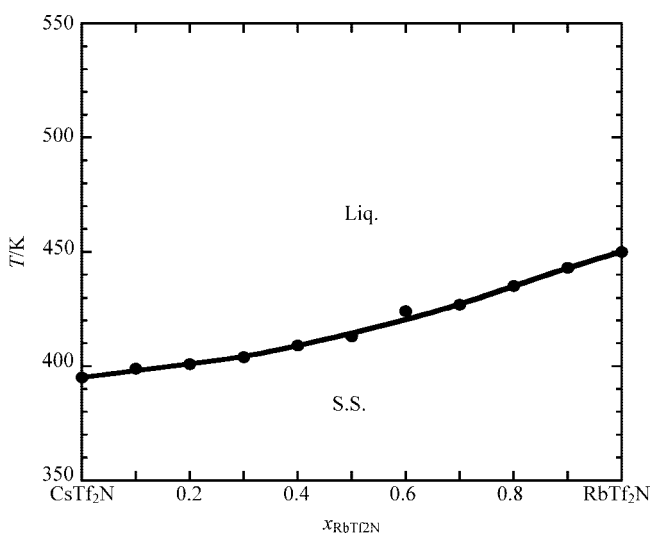
There is a peritectic point at $x_{\text{NaTf}_2\text{N}} = 0.45$ at a temperatures of 462 K. Three endothermic peaks also appear at $x_{\text{NaTf}_2\text{N}} \geq 0.45$. Similarly, it suggests the formation of a 3:1 double salt, $\text{Na}_3\text{K}(\text{Tf}_2\text{N})_4$. Figure 9 illustrates a phase diagram of $\text{NaTf}_2\text{N} + \text{CsTf}_2\text{N}$. The endothermic peak at 383 K disappears at $x_{\text{NaTf}_2\text{N}} \geq 0.75$. It suggests the formation of a 3:1 double salt, $\text{Na}_3\text{Cs}(\text{Tf}_2\text{N})_4$. A peritectic point is found at $x_{\text{NaTf}_2\text{N}} = 0.22$ with the temperature of 411 K. Table 2 summarizes the eutectic compositions and temperatures of binary MTf_2N salt mixtures. Table 3 summarizes the intermediate compounds of binary MTf_2N salt mixtures.

In the case of the $\text{KTf}_2\text{N} + \text{RbTf}_2\text{N}$ binary system, as shown in Figure 10, only one endothermic peak is observed for entire

Table 3. Intermediate Compounds of the Binary MTf_2N Salt Mixtures

system	compound
$\text{LiTf}_2\text{N} + \text{RbTf}_2\text{N}$	$\text{LiRb}(\text{Tf}_2\text{N})_2$
$\text{LiTf}_2\text{N} + \text{CsTf}_2\text{N}$	$\text{LiCs}(\text{Tf}_2\text{N})_2$
$\text{LiTf}_2\text{N} + \text{KTf}_2\text{N}$	$\text{Li}_3\text{K}(\text{Tf}_2\text{N})_4$
$\text{NaTf}_2\text{N} + \text{KTf}_2\text{N}$	$\text{Na}_3\text{K}(\text{Tf}_2\text{N})_4$
$\text{NaTf}_2\text{N} + \text{CsTf}_2\text{N}$	$\text{Na}_3\text{Cs}(\text{Tf}_2\text{N})_4$

compositions in the DSC curves. It is, thus, impossible to obtain the compositions having a lower melting point than neat RbTf_2N by the mixing of KTf_2N and RbTf_2N . The $\text{RbTf}_2\text{N} + \text{CsTf}_2\text{N}$ system, as shown in Figure 11, is similar to the $\text{KTf}_2\text{N} + \text{RbTf}_2\text{N}$ system. In this binary system, again there is only one endothermic peak at different temperatures for all mole fractions. It is concluded that these two systems form solid solutions for all mole fractions. In these systems, it is considered that there are two-phase regions where liquid and solid solution exist between liquidus and solidus. However, the regions could not be detected in this measurement.

**Figure 10.** Phase diagram of $\text{KTf}_2\text{N} + \text{RbTf}_2\text{N}$.**Figure 11.** Phase diagram of $\text{RbTf}_2\text{N} + \text{CsTf}_2\text{N}$.

It is found that the melting points are not lowered in the case of $\text{KTf}_2\text{N} + \text{RbTf}_2\text{N}$, $\text{KTf}_2\text{N} + \text{CsTf}_2\text{N}$, and $\text{RbTf}_2\text{N} + \text{CsTf}_2\text{N}$ binary systems in which two of the three heaviest alkali metal salts are mixed. When the cation sizes are close (K, 1.51 Å; Rb, 1.61 Å; Cs, 1.81 Å), the binary salt system might behave as a pseudosingle phase, although the melting temperature shifts with the composition.

Conclusions

Thermal properties of the binary MTf_2N ($M = \text{Li}, \text{Na}, \text{K}, \text{Rb}, \text{Cs}$) salt mixtures were investigated. Ten binary phase diagrams have been constructed. In the cases of the seven binary salt mixtures, the melting points are lowered to intermediate temperatures (373 to 473) K by the mixing of two single MTf_2N salts. Thus, the mixing of the alkali metal Tf_2N salt is an effective way to lower the melting temperature of alkali metal Tf_2N salts except for a few combinations.

Supporting Information Available:

The tables of data for Figures 2 to 11 are available as Supporting Information. This material is available free of charge via the Internet at <http://pubs.acs.org>.

Literature Cited

- (1) Ito, Y.; Nohira, T. Non-conventional Electrolytes for Electrochemical Applications. *Electrochim. Acta* **2000**, *45*, 2611–2622.
- (2) Galasiu, I.; Galasiu, R.; Thonstad, J. Electrochemistry of Molten Salts, In *Nonaqueous Electrochemistry*, Aurbach, D., Ed.; Marcel Dekker: New York, 1999; Chapter 9, pp 461–591.
- (3) *Ionic Liquids in Synthesis*; Holbrey, J. D., Rogers, R. D., Eds.; VCH-Wiley: Weinheim, 2002.
- (4) *Green Industrial Applications of Ionic Liquids*; Rogers, R. D., Seddon, K. R., Volkov, S., Eds.; Kluwer Academic Publishers: Norwell, MA, 2003.
- (5) *Electrochemical Aspects of Ionic Liquids*; Ohno, H., Ed.; John Wiley & Sons Inc.: New York, 2005.
- (6) Hagiwara, R.; Lee, J. S. Ionic Liquids for Electrochemical Devices. *Electrochemistry* **2007**, *75*, 23–34.
- (7) Lascaud, S.; Perrier, M.; Vallée, A.; Besner, S.; Prud'homme', J.; Armand, M. Phase Diagrams and Conductivity Behavior of Poly(Ethylene Oxide)-Molten Salt Rubbery Electrolytes. *Macromolecules* **1994**, *27*, 7469–7477.
- (8) Foropoulos, J.; DesMarteau, D. D. Synthesis, Properties, and Reactions Bis(trifluoromethyl)sulfonyl]imide, $(\text{CF}_3\text{SO}_2)_2\text{NH}$. *Inorg. Chem.* **1984**, *23*, 3720–3723.
- (9) Bonhôte, P.; Dias, A.-P.; Armand, M.; Papageorgiou, N.; Kalyanasundaram, K.; Grätzel, M. Hydrophobic, Highly Conductive Ambient-Temperature Molten Salts. *Inorg. Chem.* **1996**, *35*, 1168–1178.
- (10) Matsumoto, H.; Yanagida, M.; Tanimoto, K.; Kojima, T.; Tamiya, Y.; Miyazaki, Y. Improvement of Ionic Conductivity of Room Temperature Molten Salt Based on Quaternary Ammonium Cation and Imide Anion. *Proc. Electrochem. Soc.* **2000**, *99-41*, 186–192.
- (11) Koura, N.; Etoh, K.; Idemoto, Y.; Matsumoto, F. Electrochemical Behavior of Graphite-Lithium Intercalation Electrode in $\text{AlCl}_3\text{-EMIC-LiCl-SOCl}_2$ Room-Temperature Molten Salt. *Chem. Lett.* **2001**, *1320*, 1321.
- (12) Sakaebe, H.; Matsumoto, H. *N-Methyl-N-Propylpiperidinium Bis(Trifluoromethanesulfonyl)Imide (PP13-TFSI)* - Novel Electrolyte Base for Li Battery. *Electrochem. Commun.* **2003**, *5*, 594–598.
- (13) Xue, L.; Padgett, C. W.; DesMarteau, D. D.; Pennington, W. T. Synthesis and Structures of Alkali Metal Salts of Bis[(Trifluoromethyl)sulfonyl]Imide. *Solid State Sci.* **2002**, *4*, 1535–1545.

Received for review July 2, 2007. Accepted December 2, 2007. This work was financially supported by a Grant in Aid for Scientific Research for Priority Area "Science of Ionic Liquids" from the Japanese Ministry of Education, Culture, Sports, Science, and Technology.

JE700368R